EFFECTS OF METEOROLOGICAL CONDITIONS ON GRASSLAND FIRES IN NORTHEAST CHINA

YI, B. L.[1] – ZHANG, X. Y.[1] – LI, J.[2] – YANG, S. X.[3] – WU, G. X.[1] – SUN, J. X.[1] – ZHOU, M.[1] – DU, W. L.[4] – QI, H. G. J.[5] – AN, H. J.[1*]

[1]*ForestryCollege, Inner Mongolia Agricultural University, Hohhot, Inner Mongolia 010019, China*

[2]*Baotou Forestry and Grassland Bureau, Baotou, Inner Mongolia 014030, China*

[3]*Hulunbuir Meteorological Bureau, Hailar, Inner Mongolia 021008, China*

[4]*Institute of Grassland Research of Chinese Academy of Agricultural Sciences, Hohhot, Inner Mongolia 010010, China*

[5]*Inner Mongolia Forestry and Grassland Administration, Hohhot, Inner Mongolia 010020, China*

**Corresponding author*
e-mail: yibole88 @163.com; phone: +86-138-4814-6305; fax: +86-471-430-1330

(Received 17th May 2023; accepted 21st Jul 2023)

Abstract. Using meteorological and grassland fire data for Hulun Buir, China, from 1990 to 2019, we explored variation in meteorological factors, assessed the frequencies and areas of grassland fires, and used an autoregressive distributed lag (ARDL) model to investigate correlations between burned areas and meteorological factors. Fires in Hulun Buir grassland mainly occurred between 1990 and 1999; from 1990 to 2009, most fires occurred in Prairie Chenbarhu Banner, Xin Barag Right Banner and Xin Barag Left Banner. Grassland fires in Hulun Buir decreased significantly from 2010 to 2019. From 1990 to 2019, grassland fires mostly occurred in spring and autumn. Among the seven meteorological factors, wind speed, relative humidity and sunshine hours were most strongly correlated with burned areas. Regarding long-term and short-term effects, relative humidity had the biggest influence on burned area. The results demonstrated that ARDL models can reveal the long-term and short-term sensitivity of meteorological factors related to fire, and the ARDL econometrics method can be used effectively to study trends in grassland fire burning area.
Keywords: *Hulun Buir Grassland, grassland fire, area burned, meteorological factors, ARDL model*

Introduction

Grassland fire is an important ecological factor that has sudden and destructive effects on grassland resources and ecosystems, and rescues are extremely dangerous (Zhang et al., 2010; Finch et al., 2011; Liu et al., 2017). It is a threat to people's lives and property in pastoral areas, and it has a great influence on economic development and social stability (Liu et al., 2010; Moinuddin et al., 2018; Phillipset al., 2020). Natural grassland areas cover 41.7% of China (Su and Liu, 2004; Zhou et al., 2020), 1/3 of which are fire-prone, and 1/6 of which experience frequent fires (Tong et al., 2008). Hulun Buir Grassland is a major area in northern China that provides ecosystem services, and grassland fire here impacts economic development, social stability and livestock husbandry (Zhou et al., 2022).

Climate is an important factor determining the occurrence of grassland fire, and the temporal and spatial dynamics of grassland fire are the result of the synergistic effects of different meteorological and climate factors (Duffy et al., 2005; Nunes, 2012). Due to the

http://www.aloki.hu ● ISSN 1589 1623 (Print) ● ISSN 1785 0037 (Online)
DOI: http://dx.doi.org/10.15666/aeer/2105_43894406

influence of the earth's rotation, solar radiation received by the same area differs across seasons, and weather conditions in each month also differ, resulting in dynamic temporal and spatial changes in grassland fires (Seol et al., 2012; McKenzie et al., 2010; Syphard et al., 2017). In the North American Prairie, grassland fires are mostly concentrated in winter and early spring (Engle et al., 2001), but grassland fires in the southwest of this area are mainly concentrated in late spring and early summer (Gosz et al., 1996). Savanna grassland fires in Africa are mainly concentrated in the dry June to August period (Sheuyange et al., 2005). Grassland fires in China mostly occur in the northeast area and are concentrated in the spring and autumn (Fu et al., 2001). The Inner Mongolia Autonomous Region endures extremely frequent grassland fires, and Xilingol League and Hulun Buir City are key fire danger areas (Zhijun et al., 2009; Shabbir et al., 2019; Liu et al., 2019; Wang et al., 2023). Furthermore, the northeastern part of China is located at middle and high latitudes in the northern hemisphere and is sensitive to climate warming (He et al., 2022). During 1956–2017, the temperature in this area increased significantly, and the average temperature tendency rate was 0.327°C/10a (Wu et al., 2021), making it one of the most significant warming areas in China (He et al., 2013). The frequency of forest and grassland fires is increasing due to the direct effects of global warming (Kasischke et al., 2010; Arias et al., 2021). Prolonged high temperatures and decreased precipitation will increase the occurrence of fires in this area in the future, leading to accelerated spreading of fires (Liu, 2006; Yamamoto et al., 2016; Ying et al., 2019). Thus, it is of great significance to study the temporal and spatial dynamic characteristics of grassland fires, and the influence of meteorological factors on grassland fires in this area.

Hulun Buir, located in the northeast of the Inner Mongolia Autonomous Region in China, is a frequently burned area (Liu et al., 2017; Bao et al., 2022). Climate change is having a great impact on fires in this area (Zhang et al., 2010). Many researchers have used correlation analysis to explore correlations between different meteorological factors and fires in the Hulun Buir area (Guo et al., 2013: Liu et al., 2017; Wang et al., 2023). However, research on the nonlinear relationship between climate factors and fires in this area is scarce. Therefore, against the backdrop of climate change, it is of great significance to study the nonlinear relationship between meteorological factors and fires. In particular, grassland fire prediction and fire risk assessment in the study area can reflect the probability and damage caused by grassland fire based on future climate by considering fire occurrence frequency and fire site area.

Using historical fire and meteorological data from 1990 to 2019, we investigated the temporal and spatial dynamic characteristics of grassland fire frequency and burned area in the Hulun Buir grassland region, and predicted probable trends in grassland fire based on future climate change. Additionally, an autoregressive distributed lag (ARDL) model was established to study the occurrence of grassland fires in Hulun Buir under the influence of different meteorological factors. The results provide a theoretical basis for the prevention and control of grassland fires in this area. The findings could assist the division of grassland fire risk areas and the formulation of grassland fire prevention and control systems.

Materials and methodology

Overview of the study area

Hulun Buir grassland, located at the middle latitude of Eurasia, is one of the four largest grasslands in the world, and is the largest and best-preserved grassland in China

http://www.aloki.hu ● ISSN 1589 1623 (Print) ● ISSN 1785 0037 (Online)
DOI: http://dx.doi.org/10.15666/aeer/2105_43894406

(Zhu et al., 2007). It covers an area of 100,000 km^2 (Li et al., 2022). Hulun Buir is located in the northeast of the Inner Mongolia Autonomous Region in China, with geographical coordinates of 115°31′–126°04′ east longitude and 47°05′–53°20′ north latitude (*Fig. 1*). The Hulun Buir region is connected to Hinggan League in the south, Heilongjiang Province in the east by Nenjiang River, Russia in the north and northwest by Argun River, and Mongolia in the west and southwest. The latter border is 1733.32 km, the China-Russia border is 1051.08 km, and the China-Mongolia border is 682.24 km (Yang et al., 2022).

Hulun Buir grassland is a temperate continental climate and semi-arid area, and one of the areas most sensitive to climate change in northern China (Guo et al., 2022). With annual precipitation of about 320 mm, it is cold and dry in winter and hot and rainy in summer. The annual average temperature is -2.3°C and the altitude ranges from 200 to 1500 m. The grassland types are mainly Leymus chinensis meadow grassland, Carex mountain meadow, Stipa Baikal meadow grassland and Leymus chinensis steppe (Bian et al., 2013).

Figure 1. *Study location diagram*

Data sources

Data on grassland fires in Hulun Buir from 1990 to 2019, including occurrence time, burned area and fire grade, were obtained from the Fire Prevention Office of Forestry and the Grass Bureau of Inner Mongolia Autonomous Region.

Meteorological data were acquired from the Hulun Buir Meteorological Bureau, including daily data for seven meteorological factors: daily precipitation, daily maximum temperature (Tmax), daily minimum temperature (Tmin), daily average temperature, daily sunshine hours, daily relative humidity and 2-min average wind speed from 1990 to 2019 in Ewenki Autonomous Banner, Prairie Chenbarhu Banner, Xin Barag Right Banner, Xin Barag Left Banner, Manzhouli City and Hailar District.

Research methodology

Analysis of correlations between area burned and variables

Correlation coefficients between grassland area burned and variables of meteorological factors were calculated using the Hmisc and Performance Analytics

http://www.aloki.hu ● ISSN 1589 1623 (Print) ● ISSN 1785 0037 (Online)
DOI: http://dx.doi.org/10.15666/aeer/2105_43894406

packages in R (https://cran.r-project.org/), and dominant meteorological factors were screened out to explain the influence of meteorological changes on area burned.

ARDL model

Eviews11 (https://eviews.com/home.html) was used to calculate F statistics to test whether there was a long-term relationship between variables. The ARDL option was used to estimate the long-term coefficient between variables and the corresponding error correction model (ECM). By comparing the fitting effects of the two methods, the final fitting model was determined. The ARDL model was established to study the long-term and short-term effects of climate on the burned area of grassland.

Background of the ARDL model

ARDL models are commonly used in the field of econometrics. In econometrics, due to the changing trends in time series forecast variables (such as inflation and market value), the impacts on target responses (such as stock performance) are usually estimated. In this financial market example, past and present observations of predictive variables and response variables are associated with future response observations. These effects can be characterized as ‘short-term’ if the response fluctuates immediately when the predicted variables change, or ‘long-term’ if variables deviate but always return during the whole observation period. The ARDL model was first proposed by Pesaran et al. (1999, 2001), and its modelling process is shown in *Figure 2*. Based on work by several researchers, when there is a single long-term relationship between response and covariate, and the conditional error correction form of the covariate has no long-term relationship, the ARDL method is superior for testing cointegration. In other words, there is a simplified form in which all basic sequences are weakly exogenous and used as explanatory variables. Among these explanatory variables, there can be a mixture of I (0) and I (1) series and one or more cointegration relationships. Importantly, the ARDL method cannot be applied when one of the time series is ≥ 2-order integral (Haug, 2002; Frimpong et al., 2006). There are advantages to this model; (1) it is more stable for small samples, and even if the explanatory variables are endogenous variables, the model can generate unbiased and effective estimation results; (2) the long-term relationships of variables can be investigated by boundary cointegration tests, and it is not necessary for variables to have the same order of monotonicity; (3) the dynamic ECM can be derived by simple linear transformation, which is convenient for investigating the short-term relationships of variables (Nkoro et al., 2016).

Model building

The first step is to use the unit root test, perform Augmented Dickey-Fuller test (ADF) and Phillips-Perron (PP)tests, and determine the integer order of the sequence. If variables conform to the zero-order I(0) or the first-order I(1) simplex, then further modelling can be carried out.

The second step is to build the ARDL model as follows:

$$Y_t = \alpha_0 + \sum_{i=1}^{n} a_i Y_{t-i} + \sum_{i=0}^{m} c_i X_{t-i} + U_t \quad \text{(Eq.1)}$$

In *Equation 1*, the influence of horizontal and lagging exogenous variables on the corresponding Y at time t is expressed, along with the constant term of the coefficient

http://www.aloki.hu ● ISSN 1589 1623 (Print) ● ISSN 1785 0037 (Online)
DOI: http://dx.doi.org/10.15666/aeer/2105_43894406

effect; T is the trend term; Ut is a white noise process; N and m represent the lag order of the explained variable and the explained variable, respectively.

The cointegration test assumes that there is no stable long-term equilibrium relationship between two variables (i.e., initial hypothesis, $H_0 : \delta = 0$; alternative hypothesis, $H_0 : \delta \neq 0$ or $\delta \neq 0$). Combined with F statistics, when F statistics are less than the lower critical value, the initial hypothesis is accepted, and there is no long-term cointegration relationship between variables. If it is greater than the upper critical value, the initial hypothesis is rejected, and there is a long-term cointegration relationship between variables. If it is between two critical values, it is further judged according to the single integer order of the sequence.

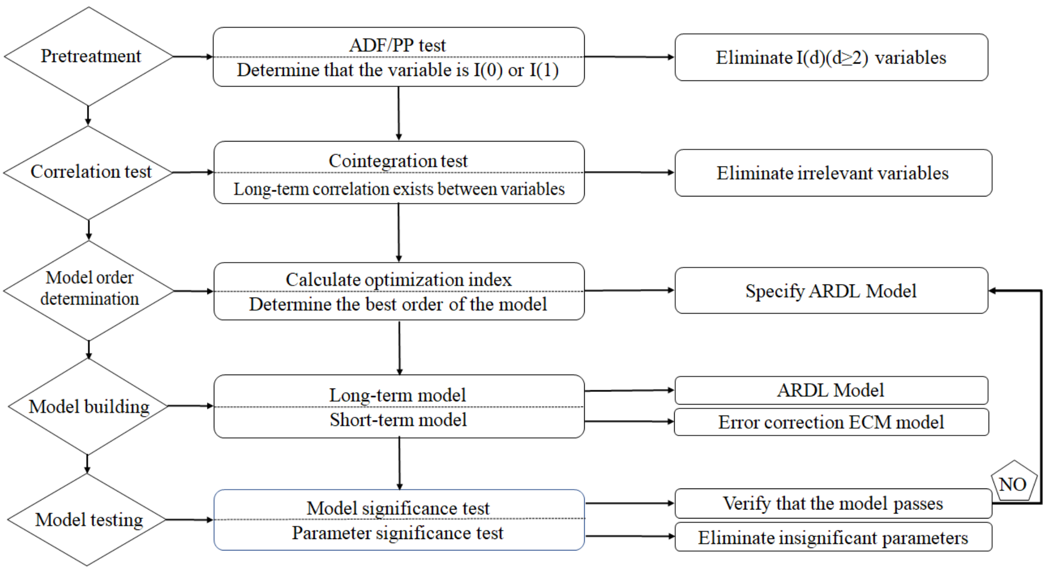

Figure 2. *Flow chart of realization of ARDL model*

After determining the long-term equilibrium relationship between variables, the model can be redefined as a short-term ECM as shown in *Equation 2*. When there is no long-term equilibrium relationship between variables and the long-term equilibrium relationship cannot be constructed, the short-term dynamic relationship and the error correction model cannot be established.

$$\nabla Y_t = \alpha_0 + \sum_{i=1}^{n-1} \alpha_i \Delta Y_{t-i} + \sum_{i=0}^{m-1} \theta_i \Delta X_{t-i} + \delta ECM_{t-1} + \varepsilon_t \qquad \text{(Eq.2)}$$

The ECM can explain the short-term fluctuation relationship of the series. α and θ respectively represent the dynamic relationship or co-integration relationship in the long-term dynamic period. The current fluctuation (ΔY_t) of the response sequence is mainly affected by the short-term fluctuation in four aspects: fluctuation of the past historical value (ΔY_{t-i}); fluctuation of the historical value of the input sequence (ΔX_{t-i}); the error of the previous period (ECM_{t-1}); and the pure random fluctuation of the current period (ε_t). ECM_{t-1} is the lag error correction factor, $\delta$is the error correction coefficient, and δ is negative.

In the third step, because there is a long-term cointegration relationship, *Equation 3* is obtained:

http://www.aloki.hu ● ISSN 1589 1623 (Print) ● ISSN 1785 0037 (Online)
DOI: http://dx.doi.org/10.15666/aeer/2105_43894406

$$\ln \text{Area burned}_t = \beta_0 + \beta_1 \ln Wind_t + +\beta_2 \ln \text{Averagetemperature}_t + \beta_3 \ln T_{max\_t} + \beta_4 \ln T_{min\_t} + \beta_5 \ln \text{Humidity}_t + \beta_6 \ln \text{Sunlight}_t + \beta_7 \ln \text{Precip}_t + v_t \tag{Eq.3}$$

In the fourth step, the final equation (*Eq. 4*) is derived from *Equation 2:*

$$\Delta \ln \text{Area burned}_t = \alpha_0 + \sum_{i=1}^{n-1} \alpha_i \Delta \ln \text{Area burned}_{t-i} + \sum_{i=0}^{m_2-1} \theta_{1i} \Delta \ln \text{Wind}_{t-i} \sum_{i=0}^{m_3-1} \theta_{2i} \Delta \ln \text{Averagetemperature}_{t-i} + \sum_{i=0}^{m_4-1} \theta_{3i} \Delta \ln T_{max\_t-i} + \sum_{i=0}^{m_5-1} \theta_{4i} \Delta \ln T_{min\_t-i} + \sum_{i=0}^{m_6-1} \theta_{5i} \Delta \ln \text{Humidity}_{t-i} + \sum_{i=0}^{m_7-1} \theta_{6i} \Delta \ln \text{Sunlight}_{t-i} + \sum_{i=0}^{m_8-1} \theta_{7i} \Delta \ln \text{Precip}_{t-i} + \delta_0 \ln \text{Area burned}_{t-1} + \delta_1 \ln \text{Wind}_{t-1} + \delta_2 \ln T_{med\_t-1} + \delta_3 \ln T_{max\_t-1} + \delta_4 \ln T_{min\_t-1} + \delta_5 \ln \text{Humidity}_{t-1} + \delta_6 \ln \text{Sunlight}_{t-1} + \delta_7 \ln \text{Precip}_{t-1} + \varepsilon_t \tag{Eq.4}$$

Results

Annual variation characteristics of grassland fire in the Hulun Buir area

Based on the interannual variation chart of grassland fires (*Fig. 3*), we concluded that there were 839 grassland fires in the Hulun Buir area from 1990 to 2019, with an average annual rate of 27.97. There were four peaks over 30 years, the highest was 110 in 1995, and occurrences decreased generally thereafter. The incidence of fires was relatively stable from 1999 to 2019, and the frequency was less than 30 per year. Overall, the number of grassland fires in this area decreased over time.

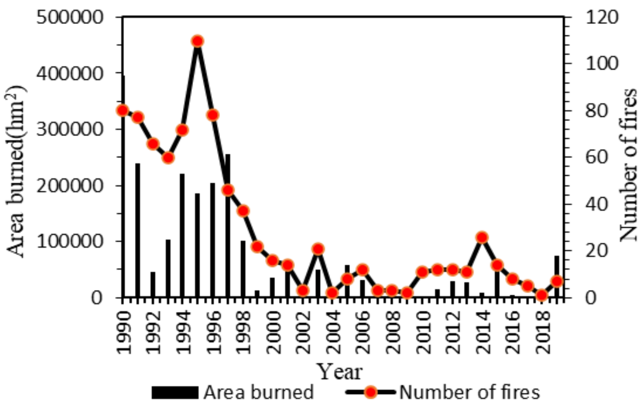

Figure 3. *Interannual variation of grassland fire*

During 1990–2019, the total burned area of Hulun Buir grassland reached 220.15×10^4 hm^2, with an average annual rate of 7.34×10^4 hm^2. The year with the smallest area of grassland fire was 2018, with a total area of 54 hm^2. The year with the largest burned area of grassland was 1990, covering 39.57×10^4 hm^2, accounting for 18% of the total burned area of grassland in 30 years. Overall, the area burned by grassland fires decreased over time, similarly to the number of grassland fires annually. After 2000 the damaged area was relatively small and stable.

According to the annual distribution of burned area of grassland fires from 1990 to 2019 (*Fig. 4*), large-scale grassland fires mainly occurred in Prairie Chenbarhu Banner, Xin Barag Right Banner and Xin Barag Left Banner from 1990 to 1999, with a maximum

http://www.aloki.hu ● ISSN 1589 1623 (Print) ● ISSN 1785 0037 (Online)
DOI: http://dx.doi.org/10.15666/aeer/2105_43894406

burned area of 2.02988 × 10^5 hm^2. From 2000 to 2009, large-scale grassland fires mainly occurred in Xin Barag Right Banner and Xin Barag Left Banner, with the largest burned area of 3.3215 × 10^4 hm^2. During 2010–2019, grassland fires covered a large area mainly in Prairie Chenbarhu Banner, with the largest burned area of 4.93 × 10^4 hm^2. Despite the different inter-annual and spatial patterns of fires during this period, from 1990 to 2019, the area of grassland fires in the Hulun Buir region decreased year by year.

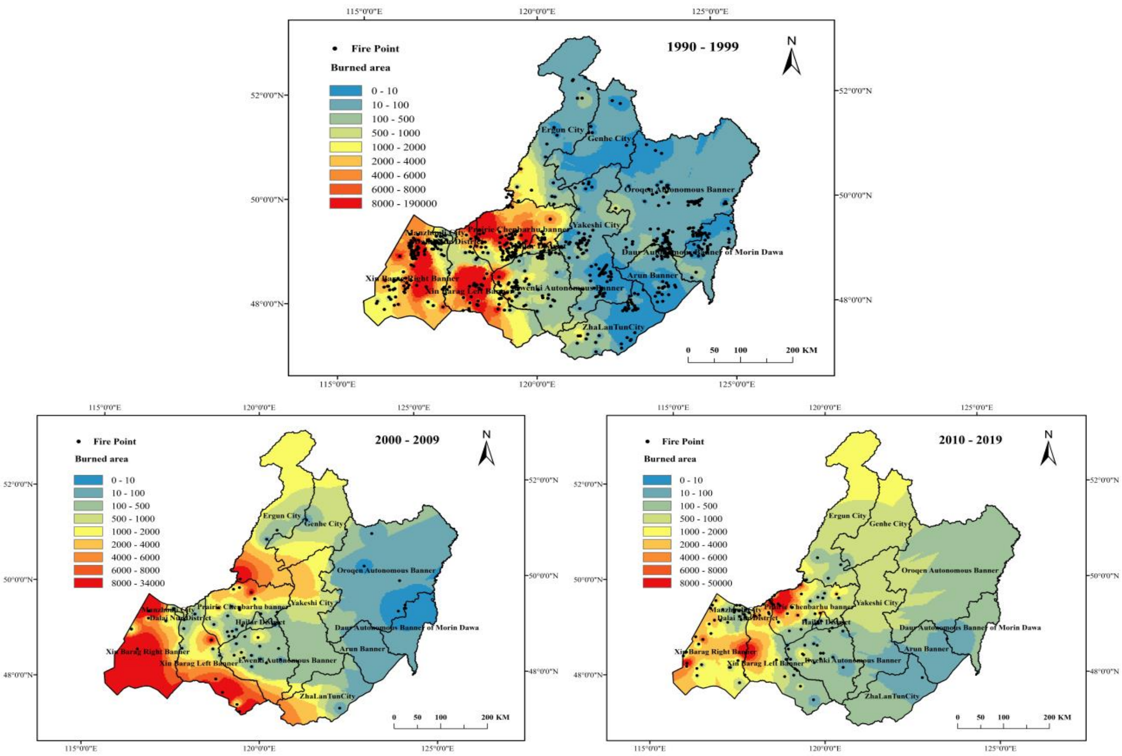

Figure 4. *Annual distribution of burned area of grassland fires from 1990 to 2019*

Monthly variation characteristics of grassland fire in the Hulun Buir area

According to monthly differences between 1990 and 2019 (January–December every year; there were no fires in February, July, August or December; *Fig. 5*), the month with the fewest grassland fires from 1990 to 2019 was January, with only one fire. The month with the most fires was April, with 289 grassland fires in April from 1990 to 2019, accounting for 34% of the total fire frequency in this area. Grassland fires occurred regularly in May and October, 255 and 122 times, respectively, accounting for 30% and 15% of the total fire frequency in this area, respectively. Therefore, the prevalence and extent of grassland fires in the Hulun Buir differed between months, occurring mainly in spring and autumn (Yi et al., 2022), consistent with changes in local meteorological elements between months (Bao et al., 2022).

Influence of climatic variables on the burned area of grassland fires

Correlation coefficients between climate parameters and burning area in three different time periods (1990–1999, 2000–2019, 2010–2019) were calculated using the R language to assess the influence of meteorological factors on burning area in different

http://www.aloki.hu ● ISSN 1589 1623 (Print) ● ISSN 1785 0037 (Online)
DOI: http://dx.doi.org/10.15666/aeer/2105_43894406

time scales (*Table 1*). The first line (grey) in the table represents the correlation coefficient, and the second line (white) represents the correlation significance p-value. The correlation coefficient between burned area and wind speed in 1990–1999 was 0.521597 and the p-value was < 0.05, indicating a significant correlation between burned area and wind speed. Similarly, from 1990 to 1999, there was a significant correlation between burned area and wind speed, relative humidity and sunshine hours. From 2000 to 2009, the burned area was significantly correlated with wind speed and relative humidity. From 2010 to 2019, the burned area showed a significant correlation with wind speed and relative humidity.

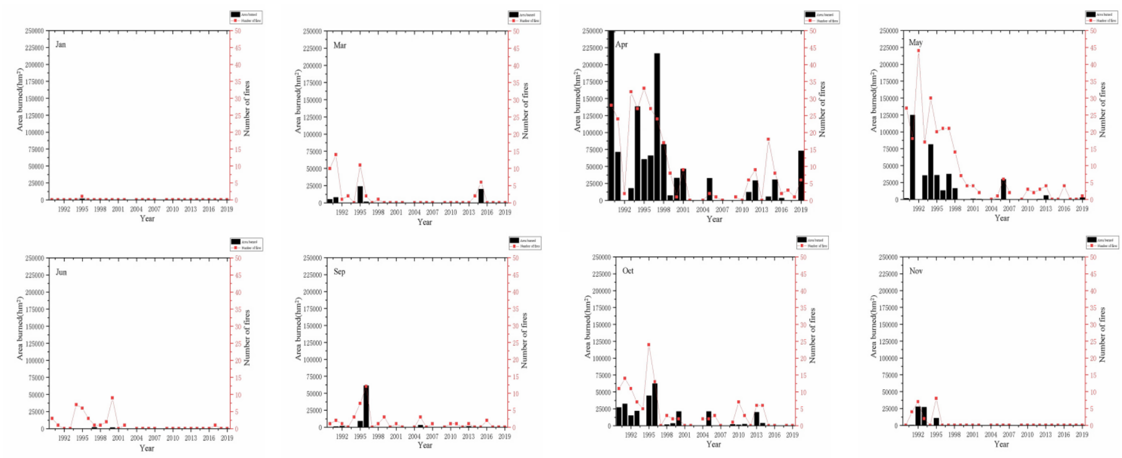

Figure 5. *Monthly variation in grassland fires*

Table 1. *Correlations between meteorological factors and burned area*

Years	Wind speed	Average temperature	Maximum temperature	Minimum temperature	Relative humidity	Sunshine hours	Precipitation
1990–99	0.521597	0.083323	0.097014	0.062971	-0.48573	0.225993	-0.16229
	1.18E-09	0.367633	0.293898	0.49628	2.15E-08	0.013461	0.077834
2000–09	0.483223	0.094943	0.099628	0.089049	-0.28266	0.063213	-0.09715
	1.78E-07	0.335343	0.311931	0.366336	0.003482	0.521767	0.324155
2010–19	0.275268	0.037009	0.04811	0.020238	-0.34878	0.140058	-0.12344
	0.002343	0.688195	0.60181	0.826337	9.46E-05	0.127078	0.179202
1990–2019	0.342678	0.057328	0.065474	0.045362	-0.28162	0.13779	-0.1052310
	0.0000	0.2780	0.2152	0.3908	0.0000	0.0089	0.0460

The first row (grey) in the table represents the correlation coefficient, and the second row (white) represents the correlation significance P value. The correlation coefficient between burned area and wind speed in 1990-1999 is 0.521597, and the p value is 0 (less than 0.05), indicating a significant correlation between burned area and wind speed. Similarly, from 1990 to 1999, there was a significant correlation between burned area and wind speed, relative humidity and sunshine time. From 2000 to 2009, the burned area was significantly correlated with wind speed and relative humidity. From 2010 to 2019, the burned area has a significant correlation with wind speed and relative humidity. Analysis of the whole experimental period shows that burned area has a significant correlation with wind speed, relative humidity, sunshine time and precipitation over 30 years.

http://www.aloki.hu ● ISSN 1589 1623 (Print) ● ISSN 1785 0037 (Online)
DOI: http://dx.doi.org/10.15666/aeer/2105_43894406

Autoregressive distributed lag (ARDL) model

Unit root test

In order to ensure consistency among time series data and to avoid pseudo-regression in the regression equation, according to the results of ADF and PP tests, stationary variables were selected for regression. Analysis revealed that p-values of all variables were < 0.05, and all variables were zero-order stationary at the 5% and 10% significance level (*Table 2*). This confirmed that the data could be used to establish an ARDL model.

By calculating the average value of each variable during the period from 1990 to 2019, and analyzing changes in burned area and seven variables in the same period (*Fig. 6*), we could assess cointegration relationships between variables. Average temperature, maximum temperature, sunshine hours and burned area showed the strongest synergistic relationships, and all had a positive cointegration relationship. There was also a synergistic relationship between minimum temperature, precipitation and burned area. However, cointegration relationships between wind speed, relative humidity and burned area could not be judged accurately due to fluctuations in variables.

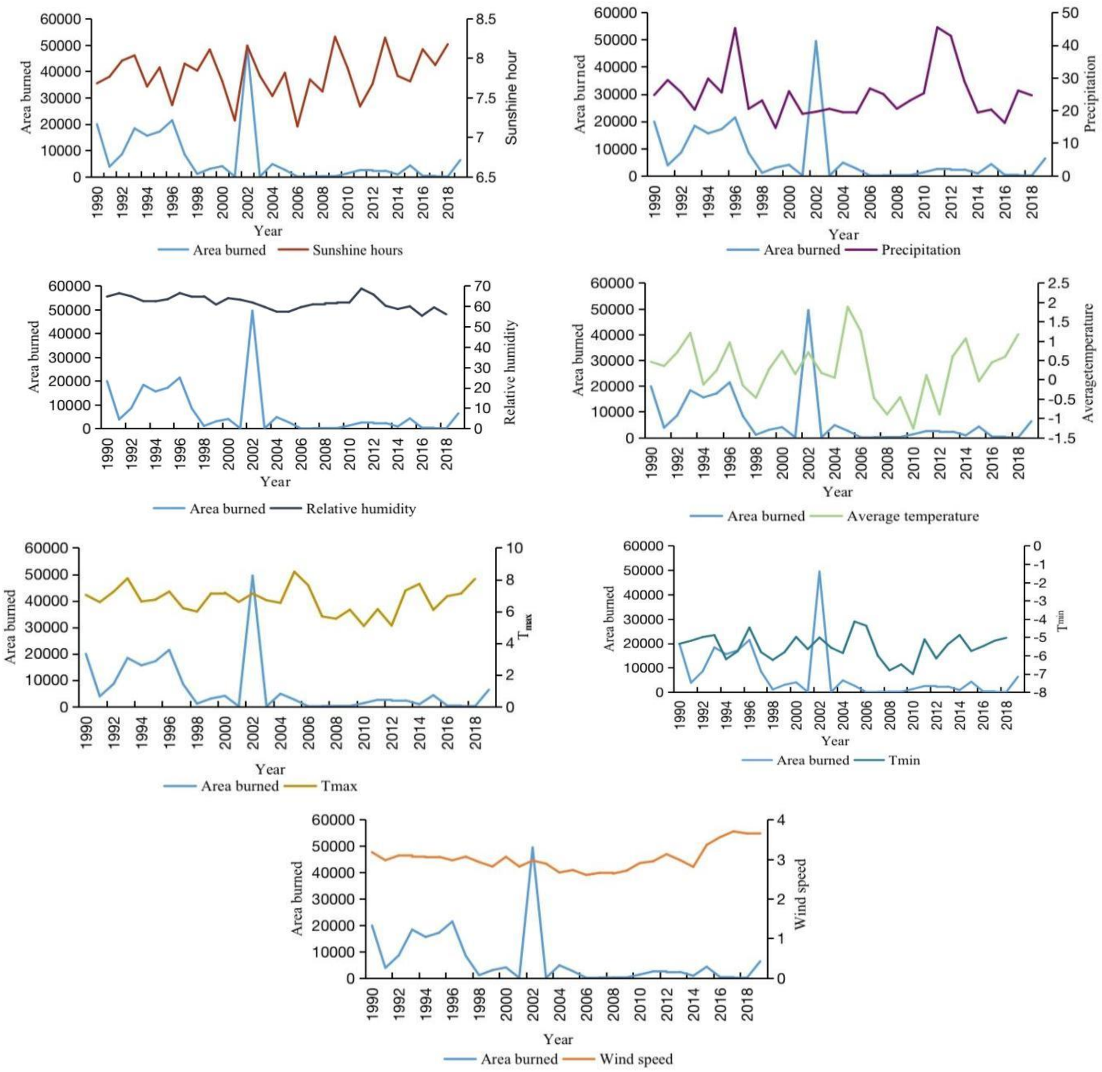

***Figure 6.** Relationship between the burned area and climate variables in HulunBuir Grassland from 1999 to 2019*

http://www.aloki.hu ● ISSN 1589 1623 (Print) ● ISSN 1785 0037 (Online)
DOI: http://dx.doi.org/10.15666/aeer/2105_43894406

Table 2. *ADF and PP test results*

	ADF test		PP test		Level of significance	
	Levels	**First differences**	**Levels**	**First differences**	**5%**	**10%**
lny	-2.797921	-14.52236	-13.53505	-76.53586	I(1)	I(1)
lnx1	-1.04224	-18.9753	-10.5868	-44.1999	I(1)	I(1)
lnx2	-2.99009	-26.8189	-5.15604	-18.2311	I(0)/I(1)	I(0)/I(1)
lnx3	-3.05706	-12.6381	-4.88357	-14.7022	I(0)/I(1)	I(0)/I(1)
lnx4	-3.0006	-25.5385	-5.29848	-18.8064	I(0)/I(1)	I(0)/I(1)
lnx5	-2.32426	-21.0843	-8.64041	-50.7079	I(1)	I(1)
lnx6	-4.01257	-22.4771	-6.07428	-31.6421	I(0)/I(1)	I(0)/I(1)

Cointegration test

Cointegration relationships can be interpreted as long-term stable equilibrium relationships between variables. Through cointegration tests, we concluded that the p-value of each statistic was < 0.05, indicating cointegration relationships between variables, and therefore long-term equilibrium relationships (*Table 3*).

Table 3. *Cointegration relationships among variables*

No. of CE(s)	Eigenvalues	Statistics	Critical values	Prob.
None *	0.549476	692.9791	159.5297	0.0000
At most 1 *	0.256384	409.9218	125.6154	0.0000
At most 2 *	0.231214	304.7598	95.75366	0.0000
At most 3 *	0.194001	211.4151	69.81889	0.0000
At most 4 *	0.155423	134.8515	47.85613	0.0000
At most 5 *	0.119509	74.88508	29.79707	0.0000
At most 6 *	0.055789	29.70241	15.49471	0.0002
At most 7 *	0.025921	9.323363	3.841466	0.0023

*Rejecting the original hypothesis at the significance level of 5%

Following cointegration tests, it is important to choose the correct lag order for y(n) in the ARDL model to avoid specification error. With a greater lag order in the model, the degree of freedom is smaller. In general, the order is determined according to the minimum value criterion of statistics. After testing, the lag order of Schwarz Bayesian statistics was the smallest, and the second lag period was selected as the order for the ARDL model (*Table 4*).

Table 4. *Optimal order of the ARDL model*

Lag	LogL	LR	FPE	AIC	SC	HQ
0	91.80623	NA	8.58e-11	-0.476172	-0.388362	-0.441228
1	805.3765	1390.651	2.14e-12	-4.166912	-3.376624	-3.852415
2	1044.043	454.2794	7.94e-13	-5.159333	-3.666567*	-4.565285
3	1165.962	226.5213	5.72e-13	-5.488423	-3.293178	-4.614821
4	1296.474	236.5521	3.93e-13	-5.866329	-2.968606	-4.713175*
5	1375.926	140.3948	3.61e-13	-5.954123	-2.353921	-4.521417
6	1441.788	113.3887	3.60e-13	-5.964707	-1.662026	-4.252448
7	1509.433	113.3818*	3.55e-13*	-5.985416*	-0.980257	-3.993605
8	1545.858	59.39757	4.20e-13	-5.828739	-0.121102	-3.557376

*Rejecting the original hypothesis at a significance level of 5%

http://www.aloki.hu ● ISSN 1589 1623 (Print) ● ISSN 1785 0037 (Online)
DOI: http://dx.doi.org/10.15666/aeer/2105_43894406

Long-term coefficients

Using the long-term coefficient, we found that the p-value of each statistical variable in the model was < 0.05, confirming significance. Moreover, the p-value of F tests for the model were < 0.05, again confirming significance. The R-squared value was 0.504179 and the fitting effect was good (*Table 5*).

After cointegration was confirmed, all variables were combined in a linear relationship and remain unchanged. Scaling this long-term relationship gave the coefficient of grassland burned area 1 (*Table 5*). According to the Schwarz Bayesian criterion, the results were estimated using the applied ARDL model. The significant long-term effects showing significance at the 5% level were wind speed, relative humidity and sunshine hours. According to these long-term elasticity effects, we estimated that a 1% change on wind speed was correlated with a 2.53% change in burned area. This long-term elasticity will not be expressed immediately, but will recover via long-term to static balance. Similarly, we predicted that when the relative humidity and sunshine hours changed by 1%, the burned area changed by 10.22% and 4.49%. From *Table 5,* we can see that the influence of burned area was significant ($p < 0.05$). This shows that burned area had a long-term impact on itself.

Table 5. *Long-term coefficients*

Selected Model: ARDL (2, 2, 0, 2, 0, 0, 0, 0)				
Variable	**Coefficient**	**Std. Error**	**t-Statistic**	**Prob.**
D(LNY(-1))	-0.430572	0.047400	-9.083814	0.0000
D(LNY(-2))	-0.272710	0.048200	-5.657879	0.0000
D(LNX1)	6.118542	1.270758	4.814875	0.0000
D(LNX1(-1))	7.206793	1.240232	5.810842	0.0000
D(LNX1(-2))	2.525008	1.160009	2.176714	0.0302
D(LNX2)	-8.661659	10.02301	-0.864177	0.3881
D(LNX3)	4.952237	4.918934	1.006770	0.3148
D(LNX3(-1))	-1.025216	0.489900	-2.092706	0.0371
D(LNX3(-2))	0.663575	0.408950	1.622630	0.1056
D(LNX4)	4.104591	5.817627	0.705544	0.4810
D(LNX5)	-10.22307	1.461605	-6.994412	0.0000
D(LNX6)	-4.487694	1.218747	-3.682220	0.0003
D(LNX7)	-0.064955	0.163657	-0.396899	0.6917
C	-0.031927	0.163332	-0.195472	0.8451
R-squared	0.504179	Mean dependent var		-0.023989
Adjusted R-squared	0.485387	S.D. dependent var		4.300978
S.E. of regression	3.085374	Akaike info criterion		5.129649
Sum squared resid.	3265.200	Schwarz criterion		5.281717
Log likelihood	-901.6423	Hannan-Quinn criter.		5.190133
F-statistic	26.82933	Durbin-Watson stat		2.181434
Prob(F-statistic)	0.000000			

Error correction model

Through ECM, we found that insignificant variables in the model were reduced, and the R^2 value was 0.586207. Compared with model 1 (long-term coefficient), SC

http://www.aloki.hu ● ISSN 1589 1623 (Print) ● ISSN 1785 0037 (Online)
DOI: http://dx.doi.org/10.15666/aeer/2105_43894406

decreases, which indicates that fitting by the model was better than that of model 1 (long-term coefficient).

According to the short-term coefficient of ECM (*Table 6*), when wind speed changed by 1% burned area changed by 3.18%, and when relative humidity changed by 1% burned area changed by 10.86%. Meanwhile, when sunshine hours changed by 1% burned area changed by 2.98%. The expected ECM lag term was negative and statistically significant, meaning that 56% of the change in grassland burned area could be explained by short-term deviation from long-term equilibrium.

Table 6. *ECM short-term coefficient*

Selected Model: ARDL (2, 1, 0, 2, 0, 0, 0, 0)				
Variable	**Coefficient**	**Std. Error**	**t-Statistic**	**Prob.**
D(LNY(-1))	-0.100413	0.052770	-1.902841	0.0579
D(LNY(-2))	-0.076680	0.043177	-1.775951	0.0766
D(LNX1)	4.984152	1.138992	4.375932	0.0000
D(LNX1(-1))	3.182454	1.094250	2.908341	0.0039
D(LNX2)	-10.13047	9.147332	-1.107478	0.2689
D(LNX3)	6.085863	4.495103	1.353887	0.1767
D(LNX3(-1))	-0.974188	0.443617	-2.196009	0.0288
D(LNX3(-2))	0.648083	0.362396	1.788330	0.0746
D(LNX4)	4.737403	5.300218	0.893813	0.3720
D(LNX5)	-10.86485	1.332310	-8.154895	0.0000
D(LNX6)	-4.698819	1.113593	-4.219512	0.0000
D(LNX7)	-0.065821	0.148944	-0.441914	0.6588
ECM(-1)	-0.559863	0.065228	-8.583224	0.0000
C	-0.021191	0.149207	-0.142024	0.8871
R-squared	0.586207	Mean dependent var		-0.023989
Adjusted R-squared	0.570524	S.D. dependent var		4.300978
S.E. of regression	2.81862	Akaike info criterion		4.948800
Sum squared resid.	2725.010	Schwarz criterion		5.100868
Log likelihood	-869.3608	Hannan-Quinn criter.		5.009284
F-statistic	37.37817	Durbin-Watson stat		2.007702
Prob(F-statistic)	0.000000			

Discussion

In the Hulun Buir grassland region, both the number of fires and the total burned area have generally decreased over the past 30 years, indicating that the local government and fire prevention management departments have achieved remarkable fire control results. However, regarding seasonal distribution, fires are still concentrated in spring and autumn, which is also the grassland fire prevention season in this area. This is caused by the dry climate in spring, less rain and more strong winds, dry grass exposed to the surface after snow melt, dry vegetation in autumn, and the reduced water content of fuel. This suggests that the climate characteristics of seasons still dominate the occurrence and spread of grassland fires. Additionally, some grasslands in Hulun Buir are located on the border between China and Mongolia, and Mongolia is sparsely populated, limiting the ability to fight forest grassland fires. Furthermore, there is less precipitation in spring and

http://www.aloki.hu ● ISSN 1589 1623 (Print) ● ISSN 1785 0037 (Online)
DOI: http://dx.doi.org/10.15666/aeer/2105_43894406

autumn, with a dry climate and numerous windy days, leading to grassland fires in these border areas, and many fires spread to Inner Mongolia (Na et al., 2018). Therefore, with global warming, precipitation reduction, temperature rise, grassland warming and drying trends, and grassland vegetation recovery upon implementation of grassland protection projects, grassland fire risk level is increasing (De Diego et al., 2019). In addition, the fire risk period in Hulunbuir grassland is shortening overall. In some years, the earlier the end of the spring fire danger period, the later the start of the autumn fire danger period, which may be due to more precipitation in the summer of that year, effectively suppressing the occurrence of autumn fires. Shortening of the fire risk period is conducive to the development of work on grassland fires, hence the fire risk period can be adjusted accordingly, but the non-fire risk period should not be ignored, and measures to prevent grassland fire in the Hulunbuir area should not be relaxed.

The results showed that the ARDL model is suitable for explaining correlations between grassland burned area and climate factors over time. The error correction model (ECM) can be used as a supplement to the co-integration model, which measures the long-term equilibrium relationship between different climatic factors and the sequence of grassland fire burned areas, while the ECM model explains short-term fluctuations. According to our ARDL analysis, relative humidity was the most important factor affecting the burned area of Hulun Buir grassland (*Table 5*). Relative humidity strongly affects the moisture content of combustible materials, and has a significant impact on the spread speed and intensity of fire (Zumbrunnen et al., 2011: Moinuddin et al., 2021). However, previous work showed that high temperature had the strongest correlation with burned area (Shabbir et al., 2019). In the present study, relative humidity had a more significant impact on burned area than high temperature. However, the influence of high temperature on burned area cannot be ignored. As temperature rises and relative humidity decreases, carbon emissions in the study area may increase, which will eventually increase the risk of fire (Pitman et al., 2007). In addition, wind speed and sunshine hours in the study area had a significant impact on the burned grassland area. The influence of wind speed on grassland fire is not only reflected in reducing the water content of combustible materials by accelerating the evaporation of water from grassland (Beer, 1991), but also in accelerating the fire spread rate, thus improving the heat transfer efficiency of unburned combustible materials (Sun et al., 2009), making fire spread faster and the burned area larger. High temperature and sufficient sunshine are mutually influencing variables act alone or together to increase plant evaporation and decrease the water content of combustible materials, thereby increasing the probability of fire (Chuvieco et al., 2004; Hennessy et al., 2005). From the results, we concluded that among the seven meteorological variables involved, relative humidity, wind speed and sunshine hours had the most significant effects on the long-term and short-term sensitivity of the ARDL model.

However, the influence of meteorological factors on grassland fires is complex and changeable, and it has an impact on the occurrence and spread of fires under the joint action of many factors (Barbero et al., 2015; Williams et al., 2019). Their relationship can be expressed as meteorological-combustible, combustible-fire and meteorological-fire. In the present study, wind speed played a leading role in the burned area of grassland in the Hulun Buir region. From 1990 to 2019, wind speed has four monthly peaks (April, May, September and October), and peaks in April and May overlap with the grassland fire season in this area. However, drought is the dominant climate factor in the surrounding areas of Hulun Buir grassland, such as Mongolian grassland and the

http://www.aloki.hu ● ISSN 1589 1623 (Print) ● ISSN 1785 0037 (Online)
DOI: http://dx.doi.org/10.15666/aeer/2105_43894406

Greater Khingan forest region (Hessl et al., 2016; Yao et al., 2017). When Mongolian grassland fires spread to Hulun Buir or Daxing ‘anling forest fires spread to Hulun Buir grassland, it is not known which meteorological factors may have the most influence.

Therefore, how different factors interact to affect the occurrence of Hulun Buir grassland fire should be the focus of future research.

Regarding climate change prediction, temperature will likely increase in the northeast of China, while precipitation and relative humidity will likely decrease (Niu and Zhai, 2012), and these changes will have an impact on the occurrence of grassland fires in northern China. In addition, the occurrence of grassland fires is not only related to meteorological factors, but also closely related to human factors (Merem et al., 2011; Guo et al., 2016; Li et al., 2017; Nagy et al., 2018), especially for the occurrence of man-made fires. However, it is difficult to predict the occurrence of man-made fires. Hulun Buir grassland is a climate-sensitive area. In this study, only the influence of different meteorological factors on the over-burned area of grassland in Hulun Buir area was considered, while human activities, combustibles and other factors were not considered. If these factors are considered simultaneously, the correlation between meteorological factors and the over-burned area of grassland may be weak.

Conclusion

In this work, the ARDL model was used to study the nonlinear correlation between the burned area of Hulun Buir grassland and different meteorological factors. Annual changes in grassland fires in this area were mainly divided into two stages; from 1990 to 1999, grassland fires in the Hulun Buir area occurred regularly, with two peaks and large overall fluctuations; from 2000 to 2019, grassland fires in the Hulun Buir area were less frequent and occurred steadily. According to the monthly changes in grassland fires in the Hulun Buir area, fires mainly occurred in April, May, September and October each year. From 1990 to 1999, grassland fires occurred frequently and covered a large area. In 2000–2009 and 2010–2019, both grassland fire frequency and burned area gradually decreased and tended to be stable. The results showed that the ARDL method can determine the long-term and short-term sensitivity of meteorological factors to fire, hence it is an effective model for studying trends in burning area for cases with high variability and short-term climate data. In terms of the influence of meteorological factors on grassland fires, relative humidity and sunshine time had obvious long-term effects on grassland fires in the Hulun Buir area, whereas wind speed, relative humidity and sunshine hours had short-term effects on grassland fires in this area.

Acknowledgements. This work was supported by the Program for improving the Scientific Research Ability of Youth Teachers of Inner Mongolia Agricultural University(Research on Meteorological Driving and Influence Prediction of Hulunbuir Grassland Fire)[grant number BR230104], Natural Science Foundation of Inner Mongolia Autonomous Region (Study on the Response Mechanism of Hulunbuir Forest and Grassland Fire Pattern to Climate Change) [grant number 2020MS03036], the Science and Technology Innovation Project of Inner Mongolia Meteorological Bureau (Prediction and Early Warning of High Forest Fire Risk in Summer Based on Passive Lightning Protection Device and Atmospheric Electric Field Instrument) [grant number: nmqxkjcx202305].

REFERENCES

[1] Arias, P., Bellouin, N., Coppola, E., Jones, R., Krinner, G., Marotzke, J., ... Zickfeld, K. (2021): Climate Change 2021: The Physical Science Basis. Contribution of Working Group I to the Sixth Assessment Report of the Intergovernmental Panel on Climate Change; Technical Summary. Cambridge University Press, Cambridge.

[2] Bao, W., Yu, F., Chang, Y., Guo, M., Zhou, F., Zhong, C. (2022): Estimation of fuel load using remote sensing data in Hulunbuir Grassland. – Natural Hazards Research 2(4): 375-383.

[3] Barbero, R., Abatzoglou, J. T., Larkin, N. K., Kolden, C. A., Stocks, B. (2015): Climate change presents increased potential for very large fires in the contiguous United States. – International Journal of Wildland Fire 24(7): 892-899.

[4] Beer, T. (1991): The interaction of wind and fire. – Boundary-Layer Meteorology 54(3): 287-308.

[5] Bian, H., Zhang, H., Zhou, D., Xu, J., Zhang, Z. (2013): Integrating models to evaluate and map grassland fire risk zones in Hulunbuir of Inner Mongolia, China. – Fire Safety Journal 61: 207-216.

[6] Chuvieco, E., Cocero, D., Riano, D., Martin, P., Martınez-Vega, J., De La Riva, J., Perez, F. (2004): Combining NDVI and surface temperature for the estimation of live fuel moisture content in forest fire danger rating. – Remote Sensing of Environment 92(3): 322-331.

[7] De Diego, J., Rúa, A., Fernández, M. (2019): Designing a model to display the relation between social vulnerability and anthropogenic risk of wild-fires in Galicia, Spain. – Urban Science 3(1): 32.

[8] Duffy, P. A., Walsh, J. E., Graham, J. M., Mann, D. H., Rupp, T. S. (2005): Impacts of large-scale atmospheric-ocean variability on Alaskan fire season severity. – Ecol. Appl15: 1317-1330.

[9] Engle, D. M., Bidwell, T. G. (2001): the response of central North American prairies to seasonal fire. – Rangeland Ecology & Management/Journal of Range Management Archives 54(1): 2-10.

[10] Finch, J., Marchant, R. (2011): A palaeoecological investigation into the role of fire and human activity in the development of montane grasslands in East Africa. Veg. Hist. – Archaeobotany 20: 109-124.

[11] Frimpong Magnus, J., Oteng-Abayie, E. F. (2006): Bounds testing approach: an examination of foreign direct investment, trade, and growth relationships. – American Journal of Applied Sciences, Forthcoming.

[12] Fu, Z. Q., Yang, Y. X., Dai, E. F. (2001): Study on dynamics of dry-grassland fire and regionalization of fire risk in Inner China. – J. Agric. Resour. Reg. Plan. 22: 18-22.

[13] Gosz, R. J., Gosz, J. R. (1996): Species interactions on the biome transition zone in New Mexico: response of blue grama (Bouteloua gracilis) and black grama (Bouteloua eripoda) to fire and herbivory. – Journal of Arid Environments 34(1): 101-114.

[14] Guo, F., Zhang, L., Jin, S., Tigabu, M., Su, Z., Wang, W. (2016): Modeling anthropogenic fire occurrence in the boreal forest of China using logistic regression and random forests. – Forests 7(11): 250.

[15] Guo, J., Yang, X., Jiang, W., Chen, F., Zhang, M., Xing, X., ... Xu, B. (2022): Sensitivity of green-up date to meteorological indicators in Hulun Buir grasslands of China. – Remote Sensing 14(3): 670.

[16] Guo, Z., Fang, W., Tan, J., Shi, X. (2013): A time-dependent stochastic grassland fire ignition probability model for Hulun Buir Grassland of China. – Chinese geographical science 23: 445-459.

[17] Haug, A. A. (2022): Temporal aggregation and the power of cointegration tests: a Monte Carlo study. – https://doi.org/10.1111/1468-0084.00025.

http://www.aloki.hu ● ISSN 1589 1623 (Print) ● ISSN 1785 0037 (Online)
DOI: http://dx.doi.org/10.15666/aeer/2105_43894406

[18] Hennessy, K., Lucas, C., Nicholls, N., Bathols, J., Suppiah, R., Ricketts, J. (2005): Climate change impacts on fire-weather in south-east Australia. – Climate Impacts Group, CSIRO Atmospheric Research and the Australian Government Bureau of Meteorology, Aspendale.
[19] Hessl, A. E., Brown, P., Byambasuren, O., Cockrell, S., Leland, C., Cook, E., ... Suran, B. (2016): Fire and climate in Mongolia (1532–2010 common era). – Geophysical Research Letters 43(12): 6519-6527.
[20] He, W., Bu, R. C., Xiong, Z. P., Hu, Y. M. (2013): Characteristics of temperature and precipitation in Northeastern China from 1961 to 2005. – Acta Ecologica Sinica 33(2): 519-531.
[21] He, X. M., Jiang, C., Wang, J., Wang, X. P. (2022): Comparison of CMIP6 and CMIP5 model performance in simulating temperature in Northeast China. – Chinese J Geophys 65(11): 4194-4207 (in Chinese).
[22] Kasischke, E. S., Verbyla, D. L., Rupp, T. S., McGuire, A. D., Murphy, K. A., Jandt, R., ... Turetsky, M. R. (2010): Alaska's changing fire regime—implications for the vulnerability of its boreal forests. – Canadian Journal of Forest Research 40(7): 1313-1324.
[23] Li, M., Wang, X., Chen, J. (2022): Assessment of grassland ecosystem services and analysis on its driving factors: a case study in Hulunbuir Grassland. – Frontiers in Ecology and Evolution 10: 25.
[24] Liu, M., Zhao, J., Guo, X., Zhang, Z., Tan, G., & Yang, J. (2017): Study on climate and grassland fire in HulunBuir, Inner Mongolia autonomous region, China. –Sensors 17(3): 616.
[25] Liu, X. P., Zhang, G. Q., Lu, J., Zhang, J. Q. (2019): Risk assessment using transfer learning for grassland fires. – Agricultural and forest meteorology 269: 102-111.
[26] Liu, X., Zhang, J., Cai, W. (2010): Information diffusion-based spatio-temporal risk analysis of grassland fire disaster in northern China. – Knowledge-Based Systems 23(1): 53-60.
[27] Liu, Y. (2006): North Pacific warming and intense northwestern US wildfires. – Geophysical Research Letters 33(21).
[28] Li, Y., Zhao, J., Guo, X., Zhang, Z., Tan, G., Yang, J. (2017): The influence of land use on the grassland fire occurrence in the Northeastern Inner Mongolia autonomous region, China. – Sensors 17(3): 437.
[29] McKenzie, D., Kennedy, M. C. (2010): Scaling Laws and Complexity in Fire Regimes. – In: McKenzie, D. et al. (eds.) The Landscape Ecology of Fire. Springer, Dordrecht, pp. 27-49.
[30] Merem, E. C., Yerramilli, S., Twumasi, Y. A., Wesley, J. M., Robinson, B., Richardson, C. (2011): The applications of GIS in the analysis of the impacts of human activities on South Texas Watersheds. – International Journal of Environmental Research and Public Health 8(6): 2418-2446.
[31] Moinuddin, K., Khan, N., Sutherland, D. (2021): Numerical study on effect of relative humidity (and fuel moisture) on modes of grassfire propagation. – Fire Safety Journal 125: 103422.
[32] Moinuddin, K. A. M., Sutherland, D., Mell, W. (2018): Simulation study of grass fire using a physics-based model: striving towards numerical rigour and the effect of grass height on the rate of spread. – International Journal of Wildland Fire 27(12): 800-814.
[33] Nagy, R. C., Fusco, E., Bradley, B., Abatzoglou, J. T., Balch, J. (2018): Human-related ignitions increase the number of large wildfires across US ecoregions. – Fire 1(1): 4.
[34] Na, L., Zhang, J., Bao, Y., Bao, Y., Na, R., Tong, S., Si, A. (2018): Himawari-8 satellite based dynamic monitoring of grassland fire in China-Mongolia border regions. – Sensors 18(1): 276.
[35] Niu, R., Zhai, P. (2012): Study on forest fire danger over Northern China during the recent 50 years. – Climatic Change 111(3): 723-736.

http://www.aloki.hu ● ISSN 1589 1623 (Print) ● ISSN 1785 0037 (Online)
DOI: http://dx.doi.org/10.15666/aeer/2105_43894406

[36] Nkoro, E., Uko, A. K. (2016): Autoregressive Distributed Lag (ARDL) cointegration technique: application and interpretation. – Journal of Statistical and Econometric Methods 5(4): 63-91.
[37] Nunes, A. N. (2012): Regional variability and driving forces behind forest fires in Portugal an overview of the last three decades (1980–2009). – Appl. Geogr 34: 576-586.
[38] Pesaran, M. H., Shin, Y., Smith, R. P. (1999): Pooled mean group estimation of dynamic heterogeneous panels. – Journal of the American statistical Association 94(446): 621-634.
[39] Pesaran, M. H., Shin, Y., Smith, R. J. (2001): Bounds testing approaches to the analysis of level relationships. – Journal of Applied Econometrics 16(3): 289-326.
[40] Phillips, N., Nogrady, B. (2020): The race to decipher how climate change influenced Australia's record fires. – Nature 577(7792): 610-613.
[41] Pitman, A. J., Narisma, G. T., McAneney, J. (2007): The impact of climate change on the risk of forest and grassland fires in Australia. – Climatic Change 84(3-4): 383-401.
[42] Seol, A., Lee, B., Chung, J. (2012): Analysis of the seasonal characteristics of forest fires in South Korea using the multivariate analysis approach. – Journal of Forest Research17(1): 45-50.
[43] Shabbir, A. H., Zhang, J. Q., Liu, X. P., Lutz, J. A., Valencia, C., Johnston, J. D. (2019): Determining the sensitivity of grassland area burned to climate variation in Xilingol, China, with an autoregressive distributed lag approach. – International Journal of Wildland Fire 28(8):628-639.
[44] Sheuyange, A., Oba, G., Weladji, R. B. (2005): Effects of anthropogenic fire history on savanna vegetation in northeastern Namibia. – Environ. Manag 75: 189-198.
[45] Su, H., Liu, G. (2004): Elementary analyses on the progress of grassland fire disaster information management technique. – Grassland of China 3: 70-72 (in Chinese).
[46] Sun, R., Krueger, S. K., Jenkins, M. A., Zulauf, M. A., Charney, J. J. (2009): The importance of fire–atmosphere coupling and boundary-layer turbulence to wildfire spread. – International Journal of Wildland Fire 18(1): 50-60.
[47] Syphard, A. D., Keeley, J. E., Pfaff, A. H., Ferschweiler, K. (2017): Human presence diminishes the importance of climate in driving fire activity across the United States. – Proceedings of the National Academy of Sciences114(52): 13750-13755.
[48] Tong, Z., Zhang, J., Liao, X. (2008): GIS-based grassland fire disaster risk management. – Journal of Basic Science and Engineering (02): 161-167 (in Chinese).
[49] Wang, Z., Huang, R., Yao, Q., Zong, X., Tian, X., Zheng, B., Trouet, V. (2023): Strong winds drive grassland fires in China. – Environmental Research Letters 18(1): 015005.
[50] Williams, A. P., Abatzoglou, J. T., Gershunov, A., Guzman-Morales, J., Bishop, D. A., Balch, J. K., Lettenmaier, D. P. (2019): Observed impacts of anthropogenic climate change on wildfire in California. – Earth's Future 7(8): 892-910.
[51] Wu, J., Sheng, Z., Du, J., Zhang, Y., Zhang, J. (2021): Spatiotemporal change patterns of temperature and precipitation in Northeast China from 1956 to 2017. – Research of Soil and Water Conservation 28(3): 340-347.
[52] Yamamoto, M., Kikuchi, T., Sakurai, H., Hayashi, R., Seki, O., Omori, T., ... Melling, L. (2021): Tropical Western Pacific hydrology during the last 6,000 years based on wildfire charcoal records from Borneo. – Geophysical Research Letters 48(18): e2021GL093832.
[53] Yang, X., Zhu, Y., Wang, B., Liu, Y. (2022): Hulun Buir Steppe Floristic Features and Vegetation Classification. – In: Yang, X. et al. (eds.) Atlas of Rangeland Plants in Hulun Buir. – Springer International Publishing, Cham, pp. 1-35.
[54] Yao, Q., Brown, P. M., Liu, S., Rocca, M. E., Trouet, V., Zheng, B., ... Wang, X. (2017): Pacific-Atlantic Ocean influence on wildfires in northeast China (1774 to 2010). – Geophysical Research Letters 44(2): 1025-1033.
[55] Yi, B. L., Yang, Y. A., Li, J. (2022): Study on the Spatial-Temporal Distribution Characteristic Law of the Grassland Fire in Hulunbuir Area. – Journal of southwest Forestry University 42(6): 131–139. (In Chinese)

http://www.aloki.hu ● ISSN 1589 1623 (Print) ● ISSN 1785 0037 (Online)
DOI: http://dx.doi.org/10.15666/aeer/2105_43894406

[56] Ying, H., Shan, Y., Zhang, H., Yuan, T., Rihan, W., Deng, G. (2019): The effect of snow depth on spring wildfires on the Hulunbuir from 2001–2018 based on MODIS. – Remote Sensing 11(3): 321.

[57] Zhang, Z. X., Zhang, H. Y., Zhou, D. W. (2010): Using GIS spatial analysis and logistic regression to predict the probabilities of human-caused grassland fires. – Journal of Arid Environments 74(3): 386-393.

[58] Zhijun, T., Jiquan, Z., Xingpeng, L. (2009): GIS-based risk assessment of grassland fire disaster in western Jilin province, China. – Stochastic Environmental Research and Risk Assessment 23: 463-471.

[59] Zhou, F., Guo, M., Zhong, C., Chang, Y., Yu, F. (2022): Spatial-temporal patterns and characteristics of grassland fire in the Hulunbuir Grassland. – Scientia Geographica Sinica 42(10): 1838-1847 (in Chinese).

[60] Zhou, W., Li, J., Yue, T. (2020): Remote Sensing Monitoring and Evaluation of Degraded Grassland in China. – Springer Science and Business Media LLC, Singapore.

[61] Zhu, Y., Qin, Z., Xu, B., Gao, M., Pei, H. (2007): An approach for desertification monitoring in Hulun Buir grassland of Inner Mongolia, China. – Proceedings of Geoinformatics 2007: Remotely Sensed Data and Information 6752: 734-742.

[62] Zumbrunnen, T., Pezzatti, G. B., Menéndez, P., Bugmann, H., Bürgi, M., Conedera, M. (2011): Weather and human impacts on forest fires: 100 years of fire history in two climatic regions of Switzerland. – Forest Ecology and Management 261(12): 2188-2199.

http://www.aloki.hu ● ISSN 1589 1623 (Print) ● ISSN 1785 0037 (Online)
DOI: http://dx.doi.org/10.15666/aeer/2105_43894406